Article

Not peer-reviewed version

Inhibitive Mechanism of Loquat Flower Isolate on Tyrosinase Activity and Melanin Synthesis in Mouse Melanoma B16 Cells

Qianqian Chen , Wenyang Tao , Jianfeng Wang * , Jingrui Li , Meiyu Zheng , Yinying Liu , Shengmin Lu * , Zhongxiang Fang

Posted Date: 28 April 2024

doi: 10.20944/preprints202404.1798.v1

Keywords: Loquat flower isolate; Tyrosinase inhibitory activity; Melanin synthesis; Melanoma B16 cells; Multi-spectroscopy; Western blotting

 doi:10.20944/preprints202404.1798.v1

Article

Inhibitive Mechanism of Loquat Flower Isolate on Tyrosinase Activity and Melanin Synthesis in Mouse Melanoma B16 Cells

Qianqian Chen [1,2], Wenyang Tao [1], Jianfeng Wang [3,*], Jingrui Li [1], Meiyu Zheng [1], Yinying Liu [4], Shengmin Lu [1,2,*] and Zhongxiang Fang [4]

[1] State Key Laboratory for Managing Biotic and Chemical Threats to the Quality and Safety of Agro-products, Zhejiang Provincial Key Laboratory of Fruit and Vegetables Postharvest and Processing Technology, Ministry of Agriculture and Rural Affairs Key Laboratory of Post-Harvest Handling of Fruits, Institute of Food Science, Zhejiang Academy of Agricultural Sciences, Hangzhou 310021, China
[2] College of Life Science, Zhejiang Normal University, Jinhua 321004, China
[3] Xingzhi College, Zhejiang Normal University, Lanxi 321100, China
[4] School of Agriculture and Food, The University of Melbourne, Parkville, Vic 3010, Australia
* Correspondence: jeffwong34@zjnu.edu.cn (J.W.); lushengmin@hotmail.com (S.L.)

Abstract: Melanin is extensively distributed in organisms and believed to be synthetized by tyrosinase (TYR), leading to aberrant coloring and skin conditions when over-produced. Loquat (*Eriobotrya japonica* (Thunb.) Lindl.) flowers contain large amounts of bioactive substances currently few studied on their suppressive capabilities to melanin synthesis. Its isolate product (LFP) was obtained by ethanol solution extraction and resin purification, of which the inhibitory mechanism on TYR activity was elaborated by enzyme kinetics and multi-spectroscopy determinations and the impact on related proteins' expression in mouse melanoma B16 cells was analyzed with Western blotting. HPLC-MS analysis indicated that LFP was identified into 137 compounds, with 12 including flavonoids (quercetin, isorhamnoin, p-coumaric acid, etc.), cinnamic acid and its derivatives as well as benzene and its derivatives owning TYR inhibitory activities. LFP inhibited TYR activity in a concentration-dependent manner with its IC50 value being 2.8 mg/mL and an anti-competitive mechanism involved altering the enzyme's conformation. LFP reduced the expression of TYR, TRP1, and TRP2 in melanoma B16 cells, hence inhibiting the synthesis of melanin. Considered collectively, LFP would be a viable option for treating hyperpigmentation caused by tyrosinase, providing a theoretical basis for the value-added utilization of loquat flower resource in beauty and aging related functional products.

Keywords: Loquat flower isolate; tyrosinase inhibitory activity; melanin synthesis; melanoma B16 cells; multi-spectroscopy; western blotting

1. Introduction

Loquat (*Eriobotrya japonica* (Thunb.) Lindl.), a fruit tree native to China, which is primarily grown in sub-tropical zones, and an evergreen that belongs to the Eriobotrya of Rosaceae family (Wu et al., 2015). Its flowering period can extend from September to February of the following year, as it yields fruit in the summer and blossoms in the winter. Flavonoids, polyphenols, and other naturally generated bioactive compounds abound in loquat blossoms (Shen, Chen, Zhu, & Yu, 2023). However, only 1-3% of all the flowers can bear fruit, which means that a majority of flowers will wither away after blossoming, resulting in even greater resource waste. Dry loquat flower is now offered as a tea drink, which has been listed in the Chinese new resource food catalog approved by China's National Health Commission, and has long been used in traditional Chinese medicine to treat coughs and phlegm. It has been discovered that loquat flower extracts (LFE) possess a wide variety of biological

 doi:10.20944/preprints202404.1798.v1

and pharmacological properties, including antibacterial, antioxidant, anti-inflammatory, and anti-tumor properties (Khouya et al., 2022; Mokhtari et al., 2023; Shen et al., 2023). However, there is no investigations that explain how LFE inhibits tyrosinase (TYR) activity and how it works to stop TYR from synthesizing melanin.

Tyrosinase, also called polyphenol oxidase, is a multipurpose oxidase that contributes to food browning through enzymatic activity and melanin biosynthesis in melanocytes. With a molecular weight of 120 kDa, this metalloenzyme contains two divalent copper ions (CuA and CuB) in its catalytically active pocket (Chen et al., 2023). Since it is the only enzyme that limits the rate at which melanin can be produced, TYR is crucial to melanin synthesis (Chen et al., 2023). TYR deploys its monophenolase activity to change L-4-hydroxyphenylalanine (L-tyrosine) into L-3,4-dihydroxyphenylalanine (L-DOPA), which is then transformed into L-dopaquinone by its diphenolase activity in cells (Shen et al., 2023). L-dopaquinone is progressively transformed and metabolized into melanin following a sequence of events and rearrangements. Excessive melanin production can result in significant esthetic issues such as hyperpigmentation, dermatosis, and melanoma (Lee et al., 2023; Shen et al., 2023). As a result, TYR inhibitors have a wide range of applications in pharmaceutical, food, cosmetic and agricultural products (Yu, Fan, & Ding, 2022; Chen et al., 2023). Kojic acid and arbutin are well-known TYR inhibitors that reduce enzymatic reactions causing foods browning and skin hyperpigmentation. Nonetheless, they have numerous side effects, including the risks of cancer, sensitization and hepatorenal damage if consumed chronically (Yu, Fan, & Ding, 2022). As a result, new, safe, and effective anti-tyrosinase natural ingredients are urgently needed.

The melanin inhibitory effect of plants and phytochemicals was reviewed by Feng, Fang, & Zhang (2022) who concluded that although many plant extracts and phytochemicals had been found to inhibit melanin production, most of the results were only proved in cellular and/or animal models and limited plant extracts had been proved effective in human trials. As far as we know, there is no report on the inhibition of loquat flower extract on tyrosinase activity and melanin synthesis. In this study, the tyrosinase inhibitory substances in loquat flowers were extracted and purified (the product was named as LFP), and its influence on *in vitro* TYR activity and action mode were investigated using UV-Vis, FT-IR, and fluorescence spectrometry. Mouse melanoma B16 cells were adopted to further investigate the melanin synthesis and its pathway affected by LFP through Western blotting. The results could provide a scientific foundation for applying loquat flower extract or isolate as a whitening agent or ingredient in functional foods and cosmetics, and encourage the value-added utilization of loquat flower resources.

2. Materials and Methods

2.1. Chemicals and Materials

Tyrosinase (EC1.14.18.1, 500 U/mg), L-DOPA, kojic acid, sodium hydroxide, copper sulphate, and phosphoric acid buffer (pH 6.8) were obtained from Yuanye Biological Technology Co., Ltd. (Shanghai, China). Methanol and acetonitrile of HPLC-MS grade were bought from Merck KgaA (Darmstadt, Germany) and formic acid (HPLC-MS grade) was from Xiya Chemical Technology (Shandong) Co., Ltd. (Linyi, China). D101 macroporous resin was supplied from Macklin Biochemical Technology Co., Ltd. (Shanghai, China). Mouse melanoma cell line B16 was got from Haotian Biotechnology Co., Ltd. (Hangzhou, China). DMEM complete culture medium, fetal bovine serum (FBS), penicillin-streptomycin solution (100×), proteinase inhibitor, trypsase and CCK8 reagent were purchased from Beijing Labgic Technology Co., Ltd. (Beijing, China). Fetal bovine serum (FBS) was obtained from Zhejiang Tianhang Biotechnology Co., Ltd. (Hangzhou, China). Tyrosinase related protein (TRP) 1, TRP2, sheep anti-rabbit second antibody, and sheep anti-mouse second antibody were from Affinity Biosciences (Ohio, USA). Deionized water was employed through the experiment. Loquat dry flowers (cv. Ninghai Bai, 5% in moisture content) were supplied by Meiqi Biotechnology Co., Ltd. (Ningbo, China).

 doi:10.20944/preprints202404.1798.v1

2.2. Preparation of LFP Sample

Using TYR inhibitory activity as the index, loquat dry flowers were extracted twice with 50% ethanol (1:20 g/mL in solid-liquid ratio, 2 h, and 50°C) after being ground and sieved through a 50-mesh screen. After pooled, extract solutions were centrifuged by a centrifuge (LXJ-IIB, Anting Scientific Instrument Factory, Shanghai, China) at 4000× *g* and room temperature, and the supernatant was collected and purified later. The loquat flower crude extract (LFE) was purified using D101 macroporous resin at a loading concentration of 40 mg/mL, loading flow rate of 3.0 BV/h, eluent concentration of 60% ethanol, and elution flow rate of 4.0 BV/h. The eluate was concentrated in a rotary evaporator (RE-2000A, Yarong Co., Ltd., Shanghai, China) and then lyophilized using a freezing drier (FD-1A-50, Xinzhi Co., Ltd., Ningbo, China) to obtain LFP.

2.3. Identification of Constituents in LFP

The LFP powder was dissolved in 70% methanol to make into a solution of 100 mg/mL before mass spectrometry detection was carried out using a Q-Exactive HF high resolution mass spectrometer (Thermo Fisher Scientific (China) Co., Ltd., Shanghai, China) equipped with a Zorbax Eclipse C18 chromatographic column (1.8 μm×2.1 mm×100 mm, Agilent Technology (China) Co., Ltd., Beijing, China). The chromatographic separation conditions were column temperature at 30°C and a flow velocity of 0.3 mL/min with mobile phase A and B being 0.1% formic acid aqueous solution and pure acetonitrile, respectively. The injection volume was 2.0 μL and automatic sampling temperature was 4°C. The mass spectrometry conditions were 3.5 KV in ion spray voltage and 325°C for ionization temperature. The scan range of mass was 100-1500 m/z.

2.4. Tyrosinase Inhibitory Activity and Kinetic Type Assays

Tyrosinase activity was determined with a MAPAD UV-3100PC spectrophotometer (Meipuda Instrument Co., Ltd., Shanghai, China) linked to an LRH-250 incubator (Shanzhi Co., Ltd., Shanghai, China) (Ha & Le, 2023). In a 96 well plate, 100 μL PBS buffer (pH 6.8), 100 μL substrate (L-DOPA, 200 g/mL), 100 μL TYR (100 U/mL), and 2 μL LFP at various concentrations (0, 1.25, 2.5, 5, 10, 20, and 40 mg/mL) were added and mixed, and then incubated at 37°C for 10 min before the absorbance of the reaction solutions were measured at 475 nm. Kojic acid was chosen as a positive control (AC).

With L-DOPA concentration remaining constant (1 mg/mL) in the reaction system, different concentrations of TYR solution (50, 100, 125, 150 U/mL) and LFP (0, 1.5, 2.5, 3.5 mg/mL) were used to investigate the type of TYR activity inhibition by LFP. The horizontal X-axis was set to TYR concentration ([E]), and the Y-axis was set to reaction velocity (v). The plotting was used to determine whether the inhibition of TYR by LFP was reversible or not (Ha & Le, 2023).

To further investigate the inhibitive mode, different concentrations of L-DOPA (0.05, 0.075, 0.1, 0.125, 0.15, 0.175, and 0.2 mg/mL) and LFP concentrations (0, 1, 2, and 3 mg/mL) were used in the reaction system. The reciprocals of substrate concentration (1/[S]) and reaction rate (1/[v]) were set on the abscissa and ordinate of the Lineweaver-Burk plot, respectively.

2.5. Determination of Copper Ion Chelating Ability of LFP

The copper ion chelating ability of LFP was assessed using the method depicted by Liu et al. (2022). Briefly, a reaction system was composed of 1.8 mL PBS (pH 6.8), 0.1 mL LFP (2.8 mg/mL), and 0.1 mL $CuSO_4$ at various concentration (0, 5, 10, 15, 20, or 25 mmol/mL). Each group of reaction solution was kept to react at 37°C for 10 min before the wavelength between 240 and 400 nm was scanned by a UV-visible spectroscopy (uv-3600plus, Shimadzu (China) Co. Ltd., Shanghai, China).

2.6. Analysis of the Secondary Structure of Tyrosinase

The FT-IR spectrum was analyzed using the method depicted by Ju et al. (2022), with minor modifications. The FT-IR spectra of TYR (100 U/mL in PBS at pH 6.8, incubated at 37°C for 10 min) in absence and presence of LFP (2.0 mg/mL) were recorded using a Thermo Nicolet-5700 spectrometer

 doi:10.20944/preprints202404.1798.v1

(Thermo Nicolet Corporation, Madison, USA) in the wavenumber range of 4000-400 cm^{-1}. The resolution was 5 cm^{-1} and the number of scans was 64.

2.7. Analysis of the Conformation Change of Tyrosinase

The reaction mixture (4 mL) included 3 mL PBS (pH 6.8), 900 μL TYR (100 U/mL), and 100 μL LFP with different concentrations (0, 0.5, 1.0, 1.5, 2.0, 2.5, 3.0, 3.5, 4.0 mg/mL). Each reaction system's fluorescence absorbance was determined using a spectrofluorometer (model F-7000, Hitachi, Japan), with the excitation wavelength, slit width of the excitation and emission spectra, voltage, and scanning speed being 275 nm, 5 nm, 600 V, and 1200 nm/s, respectively. Each sample group's emission spectrum was scanned from 300 nm to 480 nm.

The Stern-Volmer equation for fluorescence quenching is shown below.

$$\frac{F_0}{F} = 1 + K_q\tau_0[Q] = 1 + K_{sv}[Q] \quad (1)$$

where F_0 and F represent the fluorescence intensity of TYR in absence and presence of quencher (LFP), respectively. K_q is the quenching rate constant and τ_0 is the average lifetime of fluorophore without quencher. $[Q]$ means the concentration of LFP and K_{sv} denotes the Stern-Volmer quenching constant.

2.8. Cell Viability Assay

The mouse melanoma B16 cells were cultured in DMEM medium containing 10% FBS and 1% TritonX-100 in a 5% CO_2 incubator (Forma™ serie II, Thermo Fisher Scientific Inc., Waltham, MA, USA) at 37°C. In 96-well plates, cells at 1×10^4 cells/mL were inoculated and incubated for 24 h. The medium was then replaced with different concentrations of LFP (12.5, 25, 50, 100, 200, 400 μg/mL) and incubated for 48 h. After the supernatant discarded, 10 μL of CCK8 solution and 90 μL of serum-free medium were added and incubated for 2 h. Using a microplate reader (Tecan Corporation, Switzerland), the absorbance of the mixture in each well was measured at 490 nm. The viability results were expressed as the percentage of absorbance in sample cells relative to control cells (without LFP). Every sample was measured in triplicate, and each experiment was carried out at least three times.

2.9. Determination of Tyrosinase Activity and Melanin Content in Cells

Tyrosinase activity and melanin content in cells were determined using spectrophotometry. In brief, mouse B16 cells at a density of 6×10^5 cells/mL were seeded into 6-well plates, and the supernatants were discarded with a pipette after cells were incubated for 24 h (37°C, 5% CO_2), then LFP solutions (2 mL) of various concentrations (0, 25, 50, and 100 μg/mL) were added respectively before the mixtures were incubated for 48 h. The cells were lysed with 1 mL PBS (pH 6.8) containing 1% TritonX-100 using an ultrasonic crusher (JY92-IIN, Scientz Biotechnology Co., Ltd., Ningbo, China), transferred to 96-well plates, and treated with L-DOPA solution (1 mol/mL, 100 μL, 37°C) for 10 min. The absorbance of the reaction solution at 475 nm was then measured, and TYR activity was calculated as a percentage of the absorbance in sample treated cells compared to the control (without LFP). Each sample was measured in triplicate, and each experiment was repeated at least three times.

The cultured cells in the sample treated groups and the control group were rinsed three times with PBS (pH 6.8), centrifuged at 1000× *g* and 25°C to remove supernatants before being dissolved in 100 μL of 1 mol/L NaOH containing 10% DMSO, and heated in an 80°C water bath for 1 h to fully release melanin. The cell lysate was diluted with ultrapure water until it reached a volume of 400 μL. The melanin content in cell lysate was determined at the absorbance of 405 nm and expressed as a percentage of absorbance of the sample group to that of the control (without LFP). Every sample was measured in triplicate, and each experiment was carried out at least three times.

2.10. Western Blotting Analysis

The cultivated cells treated with samples (0, 50, 100 μg/mL of LFP) were used to carry out Western blotting test. The cells were lysed in a proteinase inhibitor containing PBS (pH=6.8) at 4°C

 doi:10.20944/preprints202404.1798.v1

for 20 min. Proteins were resolved by SDS polyacrylamide gel electrophoresis (SDS-PAGE) and electrophoretically transferred to a polyvinylidene fluoride (PVDF) membrane (Merk Millipore, Billerica, MA, USA). The membrane was blocked in 5% fat-free milk in PBST buffer (PBS with 0.05% Tween-20) for 1 h. After a brief wash, the membrane was incubated overnight at 4℃ with several antibodies: anti-TYR (1:1000, v/v), anti-TRP1 (1:5000), and anti-TRP2 (1:1000). A subsequent incubation with goat anti-mouse antibody (1:7500) conjugated with horseradish peroxidase was conducted at room temperature for 2 h.

Cell lysate containing 10 μg of protein was blended with 4X sample buffer (Bio-Rad, Hercules, CA, USA) and heated at 95℃ for 5 min. The heated protein was separated by SDS-PAGE (8%-12%) at 100 V for 100 min and then transferred to the PVDF membrane through a semi-dry transfer cell (Trans-Blot SD Cell; Bio-Rad, Hercules, CA, USA) at 15 V for 60 min. The membrane was blocked with 5% BSA in 1X TBST for 1 h at room temperature. After washed, the membrane was incubated with the primary antibody at 4℃ overnight and the secondary antibody at room temperature for 2 h. Specific protein bands were visualized by chemiluminescence using ECL solution (Cytiva, Tokyo, Japan) and detected by ImageQuan LAS 500 (GE Healthcare, Chicago, IL, USA) for quantification of band shadow area with Image J software (National Institutes of Health, Bethesda, MD, USA).

2.11. Statistical Analysis

All data were represented as $\bar{x} \pm$ SD. Statistical analysis of results was performed using one-way ANOVA with Tukey's correction for multiple comparisons. All data were analyzed using GraphPad Prism9.0 (GraphPad Software Inc., CA, USA).

3. Results and Discussion

3.1. Constituents of LFP

HPLC-MS analysis indicated there were 26 main classes of compounds (137 in total) identified in LFP, among which 12 including quercetin, isorhamnoin, *p*-coumaric acid, etc. in the categories of flavonoids, cinnamic acid and its derivatives as well as benzene and its derivatives (Table 1) were found to have tyrosinase inhibitory activities after a comparison with literature at home and abroad.

Table 1. Identification results of compounds in LFP with tyrosinase inhibitory activities.

Code	Compound Name	Molecular Formula	Molecular Weight	CAS Number	Retention Time (min)
		Flavonoids			
1	Quercetin (Yu et al., 2019)	$C_{15}H_{10}O_7$	302. 042 0	117-39-5	6.643
2	Isorhamnetin (Gong et al., 2020)	$C_{16}H_{12}O_7$	316. 057 7	480-19-3	7.108
3	Eriodictyol (Imen et al., 2015)	$C_{15}H_{12}O_6$	288. 063 0	209-016-4	6.894
		Cinnamic acid and its derivatives			
4	Tricoumaroyl spermidine (Zhang et al., 2022)	$C_{34}H_{37}N_3O_6$	583. 267 4	NA	9.236
5	Dicoumaramide spermidine (Zhang et al., 2022)	$C_{25}H_{31}N_3O_4$	437. 230 7	NA	9.225
6	Ethyl caffeate (Shi et al., 2005)	$C_{11}H_{12}O_4$	208. 073 2	102-37-4	9.294
7	2-Hydroxycinnamic acid (Varela et al., 2020)	$C_9H_8O_3$	164. 047 2	614-60-8	5.88
8	Coumaric acid (Varela et al., 2020)	$C_9H_8O_3$	164. 047 2	614-60-8	10.271
9	trans-4-Methoxycinnamic acid (Zheleva-Dimitrova et al., 2020)	$C_{10}H_{10}O_3$	178. 062 9	943-89-5	7.181
10	Ferulic acid (Yu & Fan, 2021)	$C_{10}H_{10}O_4$	194. 057 7	1 135-24-6	6.894

 doi:10.20944/preprints202404.1798.v1

Code	Compound Name	Molecular Formula	Molecular Weight	CAS Number	Retention Time (min)
	Benzene and its derivatives				
11	4-Methoxybenzaldehyde (Ghalla et al., 2018)	$C_8H_8O_2$	136. 052 4	123-11-5	5.952
12	p-Anisic acid (4-Methoxybenzoic acid) (Ghalla et al., 2018)	$C_8H_8O_3$	152. 047 2	100-09-4	10.034

3.2. Inhibition Type of LFP on Tyrosinase Activity

The IC50 value, representing the concentration of LFP required to reduce TYR activity by 50%, was used to reflect LFP's inhibitory ability on TYR. As shown in Figure 1(A), the TYR activity decreased as the concentration of LFP increased with its IC50 being 2.8 mg/mL, while kojic acid (AC, Figure 1(B)) had a value of 1.8 mg/mL. Although LFP had slightly lower inhibitory ability on TYR activity than kojic acid, it had the advantages of easy production, low cost, greenness, and safety compared to the latter.

The relationship between the oxidation reaction rate (v) of substrate and the concentration of TYR [E] affected by LFP is shown in Figure 1(C), which can determine whether the inhibition of LFP sample on TYR activity is reversible or not. The result showed that the slope of straight line decreased as LFP concentration increased, and all the lines passed through the origin of the coordinate axes, indicating that the inhibitory effect of LFP on TYR activity was reversible (Satish et al., 2021).

As the sample concentration increased, the straight lines in Figure 1(D) became parallel to each other, indicating that the inhibitory mode of LFP on TYR activity was anti-competitive one (Liu, Qi, & Liu, 2021). In contrast to competitive and non-competitive inhibitions, the inhibitor with anti-competitive one does not directly bind to the enzyme, but rather combines with the enzyme-substrate complex to form an enzyme-substrate-inhibitor complex (the complex cannot produce oxidized products), thereby affecting the progress of enzyme catalysis (Chen et al., 2022). Due to 26 classes of compounds present in LFP, the inhibition of LFP to TYR seems to be complicated and might be combined effects of the compounds.

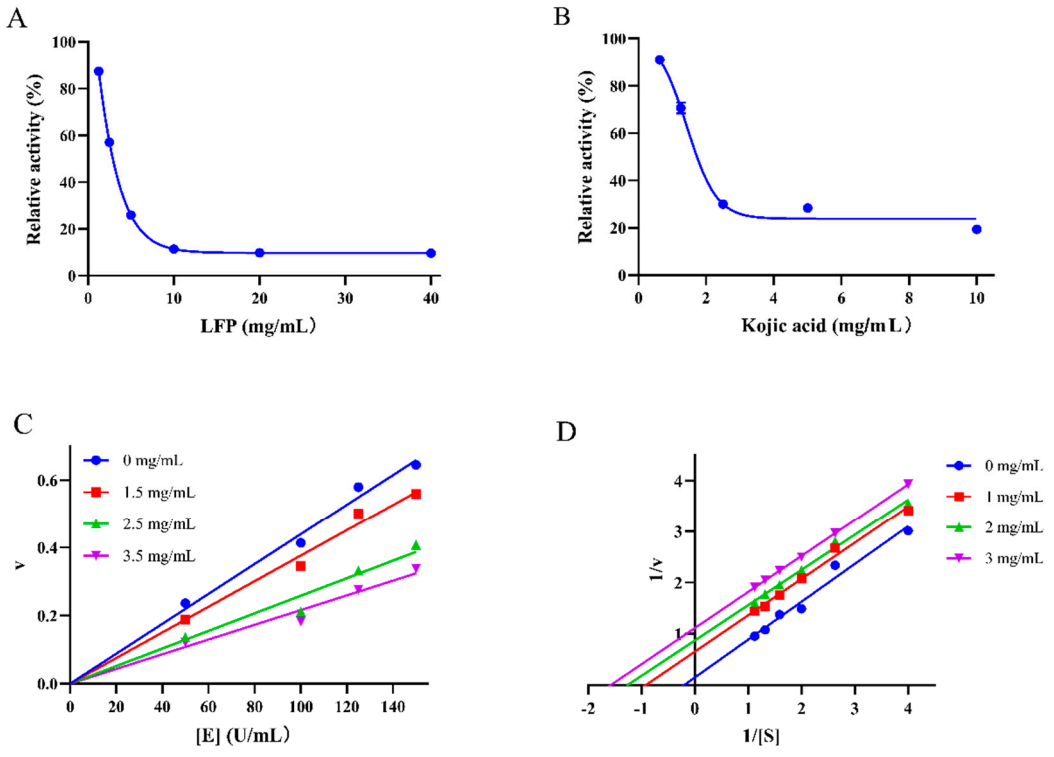

 doi:10.20944/preprints202404.1798.v1

Figure 1. Inhibitory effects of LFP (**A**) and Kojic acid (**B**) on *in vitro* activities of tyrosinase, and LFP's effect on the reaction rate of tyrosinase (**C**) and its Lineweaver Burk curves (**D**).

3.3. Copper-Ion Chelating Ability of LFP

Increasing evidence suggests that TYR inhibition is dependent in part on the inhibitor's ability to chelate the copper ions in the active site of the enzyme (Buitrago et al., 2023). The chelating property of LFP to Cu^{2+} was thus investigated. LFP had UV absorption peaks at 242 nm and 246 nm, as shown in Figure 2(A). LFP's absorption peak intensities decreased after Cu^{2+} was added. However, positions of the characteristic absorption peaks of LFP did not shift as the concentration of Cu^{2+} increased and there was no additional peak appeared, indicating that there was no direct interaction between LFP and Cu^{2+}. Although the interactions of some dietary flavonoids including quercetin had been disclosed in a pH titration solution using UV–Vis spectroscopy combined with chemometric study by Zhang et al. (2018), flavonoids present in LFP might not directly act on Cu^{2+} in active pocket of TYR. This result suggested that LFP may not inhibit tyrosinase activity through chelating copper ions at the active center of the enzyme.

3.4. Effect of LFP on Secondary Structure of Tyrosinase

Fourier transform infrared spectroscopy was used to investigate the effect of LFP on the secondary structure of tyrosinase protein, and the results were shown in Figure 2(B). The absorption peaks at 3503 and 3474 cm^{-1} in the protein were attributed to the stretching vibrations of N-H, and the contraction vibrations of $-CH_2$ in the enzyme might be responsible for the two absorption peaks at 2190 and 2160 cm^{-1}. Bands (1700-1600 cm^{-1}) at Amide I of tyrosinase occurred due to the stretching vibrations of C=O on skeleton of the protein, while those (1600-1500 cm^{-1}) at Amide II of the protein were caused by stretching vibrations of C-H and bending one of N-H in the peptide chains (Baltacioglu et al., 2015).

After added with LFP sample solution, the absorption peaks at 2931 and 2855 cm^{-1} in the enzyme might be brought about by saturated C-H stretching vibrations, while those at 2190 and 2160 cm^{-1} were shifted to 2225 and 2167 cm^{-1}, respectively, possibly due to unsaturated bonds or aromatic conjugation between the enzyme and molecules in LFP (Chen, et al., 2022). It was worth noting that the addition of LFP made all the characteristic adsorption peaks in Amide I and Amide II bands of tyrosinase appear in redshift, which indicated that interaction occurred between LFP and the enzyme caused the rearrangement of hydrogen bonding network on polypeptide chains, resulting in configuration change of tyrosinase (Liu, et al., 2022).

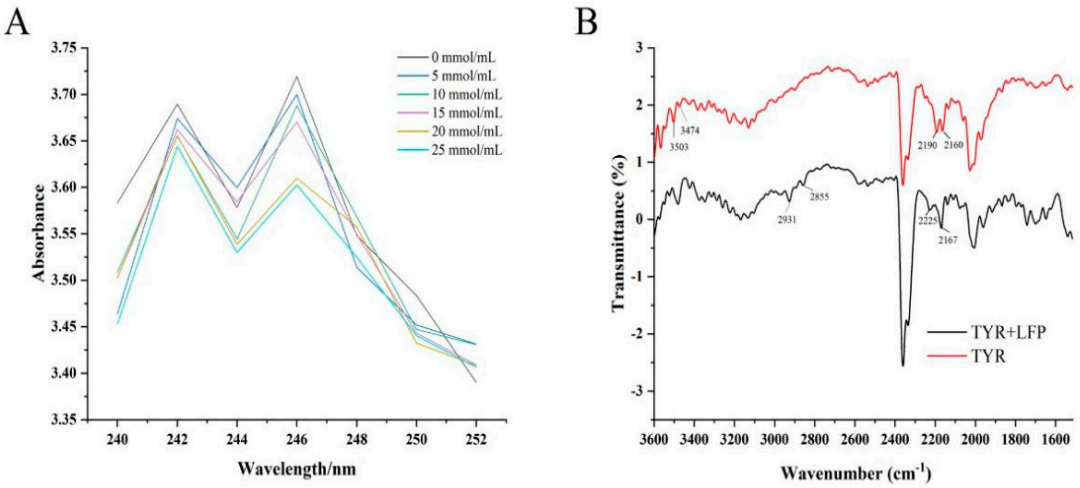

Figure 2. Effects of different concentrations of Cu^{2+} on the ultraviolet-visible spectra of LFP (**A**) and the comparison on the Fourier transform infrared spectra of tyrosinase and its mixture with LFP (**B**).

 doi:10.20944/preprints202404.1798.v1

3.5. Effect of LFP on Conformation of Tyrosinase

Tryptophan (Try) and phenylalanine (Phe) are two fluorescent chromophore groups present in tyrosinase. Try's fluorescence intensity is higher than Phe's because it has one more conjugated double bond than Phe. Moreover, Try's fluorescence spectrum may even cover Phe's because the two fluorescence spectra overlap (Haas, Hild, Kussicke, Kurre, & Lindinger, 2020). According to this phenomenon, when tyrosinase is under fluorescence spectrophotometer, there is a fluorescence peak of its own, which will rise or fall depending on whether the inhibitor added interacts with it or not. Therefore, this phenomenon can be used to assess the effect of inhibitors on tyrosinase conformation. The position of the fluorescence peak shifted from 332 to 338 nm, as shown in Figure 3(A). The result in Figure 3(B) indicated the fluorescence intensity of tyrosinase gradually decreased as the LFP concentration increased. With the addition of LFP, the fluorescence peak of TYR was redshifted, indicating a decrease in the energy required for TYR to maintain its own structure and a change in its conformation (Chen et al., 2022). The results suggested that compounds in LFP especially flavonoids may combine with TYR to quench its intrinsic fluorescence and affect the microenvironment hydrophobicity of fluorescent residues in tyrosinase (Sun et al., 2023). The combination could be due to the hydrophobic interaction between flavonoids in LFP and amino acid residues in tyrosinase, resulting in the exposure of protein polypeptide chains to the environment, thereby inhibiting the catalytic reaction of tyrosinase (Lai et al., 2023). There was a linear relationship between F_0/F and [*Q*] in Figure 3(C), and the *K*sv value decreased with increasing temperature (296 K-303 K). As a result, the fluorescence quenching of tyrosinase by LFP was determined to be static quenching (Jia et al., 2023). In summary, LFP can bind to tyrosinase when tyrosinase and LFP coexist and its activity is significantly inhibited since its fluorescence intensity decreases dramatically as LFP content increases.

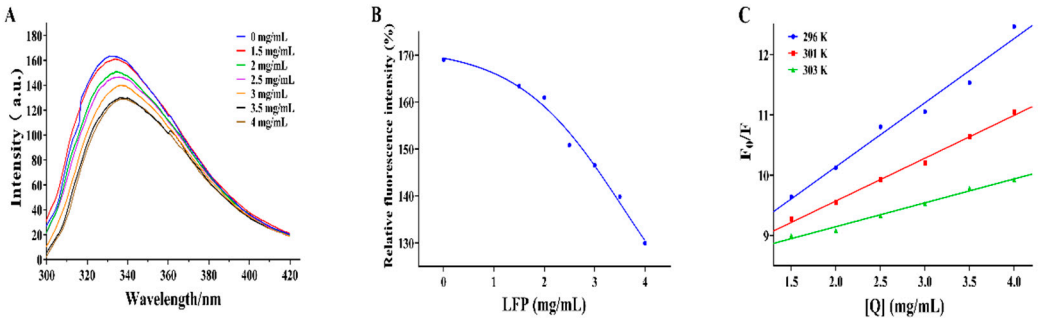

Figure 3. Effect of different concentrations of LFP on the fluorescence intensity of tyrosinase (**A**), the relative fluorescence intensity changed with LFP concentrations (**B**), and Stern-Volmer curve graphs of fluorescence quenching of tyrosinase by LFP (**C**).

3.6. Effect of LFP on the Viability of Mouse Melanoma B16 Cells

The effect of LFP on the viability of mouse melanoma B16 cells was assessed by the CCK8 method (Figure 4A). Result showed that LFP solution at less than 200 μg/mL was non-toxic to the cells, with a survival rate more than 80% (Gasowska-Bajger & Wojtasek, 2023). However, the viability of the cells decreased in a dose-dependent manner as the concentration of LFP increased. Since LFP less than 200 μg/mL had no cytotoxic effect on B16 melanoma cells, 0-200 μg/mL LFP were used in the following experiments.

 doi:10.20944/preprints202404.1798.v1

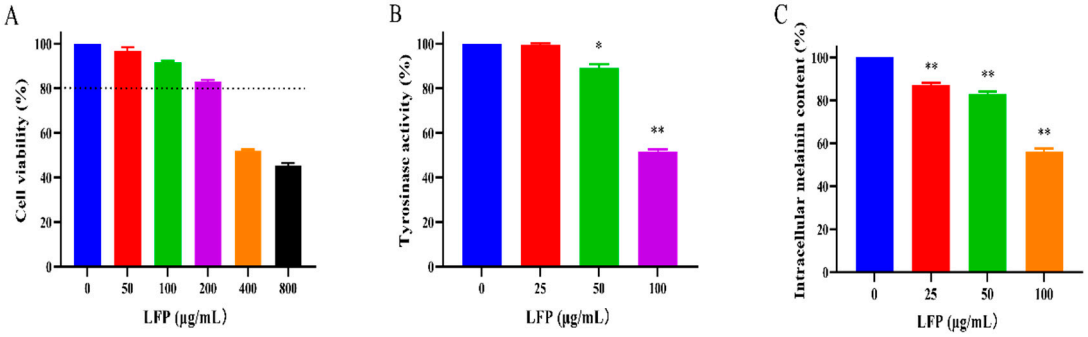

Figure 4. Effect of LFP on the vitality (**A**), TYR activities (**B**), and melanin contents (**C**) of mouse melanoma B16 cells. * and ** indicate $P < 0.05$ and $P < 0.01$, respectively, compared to the model.

3.7. Effect of LFP on Tyrosinase Activity and Melanin Synthesis in B16 Cells

To evaluate the effect of LFP on melanin production, we measured intracellular TYR activity and melanin content in B16 cells after treated with LFP. At different concentrations (25, 50, and 100 μg/mL), LFP inhibited TYR activity and melanin formation in a dose-dependent manner, as shown in Figure 4(B). When the concentration of LFP was 50 μg/mL, TYR activity in the cells began to significantly decrease ($P < 0.05$) compared to that of the blank control group (without LFP). The activity of intracellular TYR was significantly reduced ($P < 0.01$) to 51.6% when LFP concentration was 100 μg/mL. This demonstrated that LFP treatment at 50 μg/mL or higher significantly inhibited tyrosinase activity in mouse melanoma B16 cells.

Figure 4(C) showed LFP treatment (25-100 μg/mL) significantly reduced melanin content in B16 cells compared to the blank control ($P < 0.01$). The relative contents of intracellular melanin were decreased to 82.8% and 56.2% after the cells were treated with 50 and 100 μg/mL LFP, respectively. This indicated that LFP had a significant inhibition effect on melanin synthesis in mouse melanoma B16 cells. Based on the results, it was concluded that LFP could reduce the synthesis of melanin through inhibiting B16 intracellular TYR activity.

3.8. Western Blotting Results

As a rate limiting enzyme in melanin synthesis, TYR directly affects the reaction rate of melanin synthesis. TRP2 is involved in the chemical reaction that converts dopamine pigment to 5,6-dihydroxyindole-3-carboxylic acid (DHICA) during melanin synthesis, while TRP1 participates in transformation of DHICA to 5,6-indolequinone carboxylic acid (IQCA) as well as the oxidation reaction that produces true melanin (Deng, Zhao, He, & Tian, 2023; Jenkins, Vitousek, & Safran, 2013; Suzuki et al., 2023). These three proteins are closely related to melanin synthesis and located downstream in the protein pathway of melanin synthesis. As shown in Figure 5(A), there was no significant difference in the expression of TYR after 100 μg/mL LFP treatment compared to 25 μg/mL kojic acid treatment ($P > 0.05$). However, LFP inhibited TYR expression in a concentration-dependent manner and the inhibition was significant by 100 μg/mL LFP compared to 50 μg/mL LFP ($P < 0.01$), which corresponded to the trend in Figure 4(B). When compared to the blank control, the experimental group treated with 50 μg/mL LFP had significantly reduced expression of TYR ($P < 0.01$), while that treated with 100 μg/mL LFP had an extremely significant decrease in TYR expression ($P < 0.0001$). The findings showed that LFP at concentration more than 50 μg/mL had a significant inhibitory effect on TYR expression in B16 cells.

TRP1 expression levels were decreased extremely significantly ($P < 0.0001$) and significantly ($P < 0.01$) after 50 and 100 μg/mL LFP were administered to the cells, respectively, as shown in Figure 5(B). Particularly, the 50 μg/mL LFP treatment resulted in lower TRP1 expression than the positive control (25 μg/mL kojic acid). TRP1 expression in 50 μg/mL LFP treated group was significantly lower than that in 100 μg/mL LFP treated one ($P < 0.01$), which might need more investigation to reveal the potential account. TRP2 expression levels were affected by LFP treatment in a concentration-

 doi:10.20944/preprints202404.1798.v1

dependent manner (Figure 5(C)). The TRP2 expression was significantly reduced in both the 50 μg/mL and 100 μg/mL LFP treatments compared to the blank control ($P < 0.05$ and $P < 0.01$, respectively).

In summary, LFP inhibited intracellular tyrosinase activity and melanin synthesis primarily through suppressing the expressions of TYR, TRP1 and TRP2. However, due to 12 components in LFP with reported tyrosinase inhibitory activities (Table 1) identified in this study, their inhibitory abilities to TYR activity and melanin synthesis (underlying pathways) and synergistic/counteractive action modes await to be validated in future.

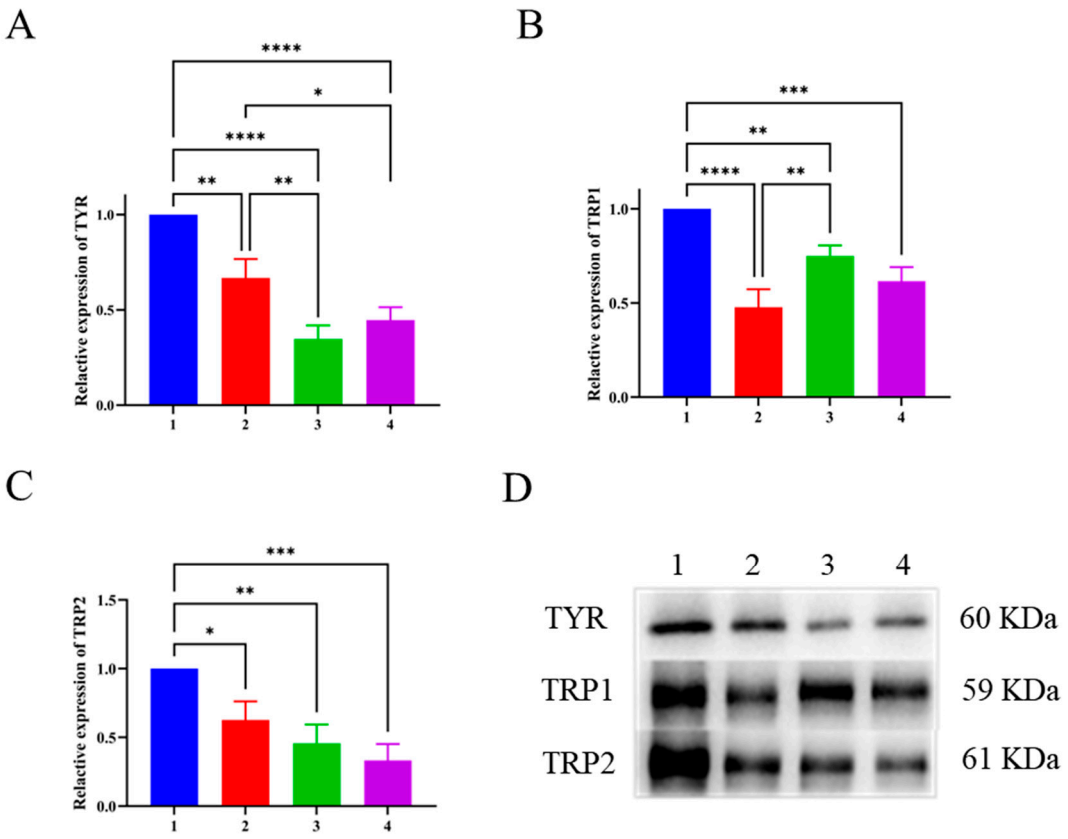

Figure 5. Effects of LFP on TYR (**A**), TRP1 (**B**) and TRP2 (**C**) expressions in mouse melanoma B16 cells and their electrophoregrams (**D**). The numbers on the abscissas and the electrophoregram represent groups of the blank control (without LFP, 1), 50 μg/mL LFP treatment (2), 100 μg/mL LFP treatment (3) and the positive control (25 μg/mL kojic acid, 4), respectively. *, **, ***, and **** indicate the significant difference level at $P < 0.05$, $P < 0.01$, $P < 0.001$, and $P < 0.0001$, respectively.

4. Conclusions

Loquat flower isolate had considerable TYR activity inhibitory ability with its IC_{50} value being 2.8 mg/mL, which was slightly higher than that of kojic acid (1.8 mg/mL). LFP inhibited TYR activity in an anti-competitive inhibition and had no chelating effect on copper-ions. The inhibition of LFP on TYR activity was achieved by affecting the secondary structure and conformation of the enzyme. At the cellular level, it was demonstrated that tyrosinase activity in mouse melanoma B16 cells was significantly inhibited after the cells were treated with LFP at concentrations above 50 μg/mL ($P < 0.05$). The cells had significantly reduced synthesis rate of melanin after treated with LFP at more than 25 μg/mL ($P < 0.01$). Western blotting results indicated LFP inhibited melanin synthesis through decreasing the expressions of TYR, TRP1 and TRP2. The findings provided a preliminary scientific foundation for using loquat flower isolate as a natural tyrosinase inhibitor and potential whitening ingredient in functional foods and cosmetics and more detailed studies such as underlying pathways

 doi:10.20944/preprints202404.1798.v1

in melanin synthesis affected by individual components present in LFP and their possible synergistic action mechanism are needed.

Author Contributions: Qianqian Chen: Data curation, Formal analysis, Software, Visualization, Roles/Writing - original draft. Wenyang Tao: Methodology, Validation, Writing - review & editing. Jianfeng Wang: Investigation, Resources, Supervision. Jingrui Li: Formal analysis, Investigation, Visualization. Meiyu Zheng: Investigation, Methodology, Resources. Yinying Liu: Methodology, Software, Visualization. Shengmin Lu: Funding acquisition, Resources, Supervision, Writing - review & editing. Zhongxiang Fang: Resources, Supervision, Writing - review & editing.

Acknowledgments The authors acknowledge the State Key Laboratory for Managing Biotic and Chemical Threats of the Quality and Safety of Agro-products (2021DG700024-ZZ202210) for the financial support of this research.

Conflicts of Interest The authors of the present work declare no conflict of interest.

Abbreviations: LFE: Loquat flower (crude) extract; LFP, Loquat flower isolate product; TYR, Tyrosinase; TRP1, Tyrosinase related protein 1; TRP2, Tyrosinase related protein 2; L-DOPA, L-3,4-dihydroxyphenylalanine; FBS, Fetal bovine serum.

References

Baltacioglu, H., Bayindirli, A., Severcan, M.,& Severcan, F. (2015). Effect of thermal treatment on secondary structure and conformational change of mushroom polyphenol oxidase (PPO) as food quality related enzyme: A FTIR study. Food Chemistry, *187*:263-269. https://doi.org/10.1016/j.foodchem.2015.04.097

Buitrago, E., Faure, C., Carotti, M., Bergantino, E., Hardre, R., Maresca, M., Philouze, C., Vanthuyne, N., Boumendjel, A., Bubacco, L., du Moulinet d'Hardemare, A., Jamet, H., Reglier, M., & Belle, C. (2023). Exploiting HOPNO-dicopper center interaction to development of inhibitors for human tyrosinase. *Eur J Med Chem, 248*, Article 115090. https://doi.org/10.1016/j.ejmech.2023.115090

Chen, Q., Shang, C., Han, M., Chen, C., Tang, W., & Liu, W. (2023). Inhibitory mechanism of scutellarein on tyrosinase by kinetics, spectroscopy and molecular simulation. *Spectrochim Acta A Mol Biomol Spectrosc, 296*, Article 122644. https://doi.org/10.1016/j.saa.2023.122644

Chen, W., Shi, X., Xu, W., McClements, D. J., Liu, X., & Liu, F. (2022). Effects of different polyphenols on the structure and properties of sodium caseinate films mediated by tyrosinase. Journal of Agriculture and Food Research, 10, Article 100395. https://doi.org/10.1016/j.jafr.2022.100395

Deng, B., Zhao, J., He, M., & Tian, S. (2023). Curcumin treatment enhances bioactive metabolite accumulation and reduces enzymatic browning in soybean sprouts during storage. *Food Chem X, 17*, Article 100607. https://doi.org/10.1016/j.fochx.2023.100607

Feng, D., Fang, Z., & Zhang, P. (2022). The melanin inhibitory effect of plants and phytochemicals: A systematic review. *Phytomedicine, 107*, Article 154449. https://doi.org/10.1016/j.phymed.2022.154449

Gasowska-Bajger, B., & Wojtasek, H. (2023). Oxidation of baicalein by tyrosinase and by o-quinones. *Int J Biol Macromol, 231*, Article 123317. https://doi.org/10.1016/j.ijbiomac.2023.123317

Ghalla, H., Issaoui, N., Bardak, F., & Atac, A. (2018). Intermolecular interactions and molecular docking investigations on 4-methoxybenzaldehyde. *Computational Materials Science, 149*, 291-300. https://doi.org/10.1016/j.commatsci.2018.03.042

Gong, G., Guan, Y. Y., Zhang, Z. L., Rahman, K., Wang, S. J., Zhou, S., Luan, X., & Zhang H. (2020) Isorhamnetin: A review of pharmacological effects. *Biomedicine Pharmacotherapy, 128*, Article 110301. https://doi.org/10.1016/j.biopha.2020.110301

Ha, A. C., & Le, T. M. (2023). Improvement of anti-tyrosinase activity in potential skin whitening products by combining herbal extracts and reducing their tannin content by collagen fibre adsorption. *South African Journal of Botany, 155*, 118-126. https://doi.org/10.1016/j.sajb.2023.02.020

Haas, B., Hild, M. B., Kussicke, A., Kurre, A., & Lindinger, A. (2020). Fluorescence contrast improvement by polarization shaped laser pulses for autofluorescent biomolecules. *Optik, 207*, Article 163777. https://doi.org/10.1016/j.ijleo.2019.163777

Imen, M. B., Chaabane, F., Nadia, M., Soumaya, K. J., Kamel, G., & Leila, C. G. (2015). Anti-melanogenesis and antigenotoxic activities of eriodictyol in murine melanoma (B16-F10) and primary human keratinocyte cells. *Life Sciences, 135*, 173-178. https://doi.org/10.1016/j.lfs.2015.06.022

Jenkins, B. R., Vitousek, M. N., & Safran, R. J. (2013). Signaling stress? An analysis of phaeomelanin-based plumage color and individual corticosterone levels at two temporal scales in North American barn swallows, Hirundo rustica erythrogaster. *Horm Behav, 64* (4), 665-672. https://doi.org/10.1016/j.yhbeh.2013.08.006

Jia, Y., Yan, X., Li, X., Zhang, S., Huang, Y., Zhang, D., Li, Y., & Qi, B. (2023). Soy protein-phlorizin conjugate prepared by tyrosinase catalysis: Identification of covalent binding sites and alterations in protein structure and functionality. *Food Chem, 404* (Part A), Article 134610. https://doi.org/10.1016/j.foodchem.2022.134610

Ju, X., Cheng, S., Li, H., Xu, X., Wang, Z., & Du, M. (2022). Tyrosinase inhibitory effects of the peptides from fish scale with the metal copper ions chelating ability. *Food Chem, 390*, 133146. https://doi.org/10.1016/j.foodchem.2022.133146

Khouya, T., Ramchoun, M., Elbouny, H., Hmidani, A., Bouhlali, E. D. T., & Alem, C. (2022). Loquat (*Eriobotrya japonica* (Thunb) Lindl.): Evaluation of nutritional value, polyphenol composition, antidiabetic effect, and toxicity of leaf aqueous extract. *J Ethnopharmacol, 296*, Article 115473. https://doi.org/10.1016/j.jep.2022.115473

Lai, X., Zhang, G., Deng, S., Huang, Z., Peng, J., Zhang, G., Su, L., He, W., Wu, Y., Ding, N., Zhang, Z., & Lai, W. (2023). Synergistic dual-mechanism fluorescence quenching immunochromatographic assay based on Fe-polydopamine submicrobeads for sensitive detection of enrofloxacin. *Chemical Engineering Journal, 454*. Article 140444. https://doi.org/10.1016/j.cej.2022.140444

Lee, J., Jeong, Y., Jin Jung, H., Ullah, S., Ko, J., Young Kim, G., Yoon, D., Hong, S., Kang, D., Park, Y., Chun, P., Young Chung, H., & Ryong Moon, H. (2023). Anti-tyrosinase flavone derivatives and their anti-melanogenic activities: Importance of the beta-phenyl-alpha,beta-unsaturated carbonyl scaffold. *Bioorg Chem, 135*, Article 106504. https://doi.org/10.1016/j.bioorg.2023.106504

Liu, H., Qi, Z., & Liu, C. (2021). Inhibition mechanisms of humic acid and protein on the degradation of sulfamethazine by horseradish peroxidase. *Colloids and Surfaces A: Physicochemical and Engineering Aspects, 629*, Article 127473. https://doi.org/10.1016/j.colsurfa.2021.127473

Liu, L., Li, J., Zhang, L., Wei, S., Qin, Z., Liang, D., Ding, B., Chen, H., & Song, W. (2022). Conformational changes of tyrosinase caused by pentagalloylglucose binding: Implications for inhibitory effect and underlying mechanism. *Food Res Int, 157*, Article 111312. https://doi.org/10.1016/j.foodres.2022.111312

Mokhtari, I., Moumou, M., Harnafi, M., Milenkovic, D., Amrani, S., & Harnafi, H. (2023). Loquat fruit peel extract regulates lipid metabolism and liver oxidative stress in mice: *In vivo* and *in silico* approaches. *J Ethnopharmacol, 310*, Article 116376. https://doi.org/10.1016/j.jep.2023.116376

Satish, L., Santra, S., Tsurkan, M. V., Werner, C., Jana, M., & Sahoo, H. (2021). Conformational changes of GDNF-derived peptide induced by heparin, heparan sulfate, and sulfated hyaluronic acid - Analysis by circular dichroism spectroscopy and molecular dynamics simulation. *Int J Biol Macromol, 182*, 2144-2150. https://doi.org/10.1016/j.ijbiomac.2021.05.194

Shen, Z., Chen, J., Zhu, J., & Yu, H. (2023). Changes of bioactive composition and concentration in loquat flower extracted with water/Chinese Baijiu. *Heliyon, 9* (4), e14701. https://doi.org/10.1016/j.heliyon.2023.e14701

Shi, Y., Chen, Q. X., Wang, Q., Song, K. K., & Qiu, L. (2005). Inhibitory effects of cinnamic acid and its derivatives on the diphenolase activity of mushroom (*Agaricus bisporus*) tyrosinase. *Food Chemistry, 92*, 707-712. https://doi.org/10.1016/j.foodchem.2004.08.031

Sun, Q., Guo, Y., Li, X., Luo, X., Qiu, Y., & Liu, G. (2023). A tyrosinase fluorescent probe with large Stokes shift and high fluorescence enhancement for effective identification of liver cancer cells. *Spectrochim Acta A Mol Biomol Spectrosc, 285*, Article 121831. https://doi.org/10.1016/j.saa.2022.121831

Suzuki, T., Hoshino, M., Nishimura, M., Ide, F., Kusama, K., Sakashita, H., & Kikuchi, K. (2023). A rare case of melanin-pigmented dentinogenic ghost cell tumor. *Journal of Oral and Maxillofacial Surgery, Medicine, and Pathology, 35* (4), 335-340. https://doi.org/10.1016/j.ajoms.2022.12.001

Varela, M. T., Ferrarini, M., Mercaldi, V. G., Sufi, B. da S., Padovani, G., Nazato, L. I. S., & Fernandes, J. P. S. (2020). Coumaric acid derivatives as tyrosinase inhibitors: Efficacy studies through *in silico*, *in vitro* and *ex vivo* approaches. *Bioorganic Chemistry, 103*, Article 104108. https://doi.org/10.1016/j.bioorg.2020.104108

Wu, S. K., Zhang, N., Shen, X. R., Mei, W. W., He, Y., & Ge, W. H. (2015). Preparation of total flavonoids from loquat flower and its protective effect on acute alcohol-induced liver injury in mice. *J Food Drug Anal, 23* (1), 136-143. https://doi.org/10.1016/j.jfda.2014.07.001

 doi:10.20944/preprints202404.1798.v1

Yu, Q., & Fan, L. (2021). Understanding the combined effect and inhibition mechanism of 4-hydroxycinnamic acid and ferulic acid as tyrosinase inhibitors. *Food Chemistry, 2021, 352*, Article 129369. https://doi.org/10.1016/j.foodchem.2021.129369

Yu, Q., Fan, L., & Ding, Z. (2022). The inhibition mechanisms between asparagus polyphenols after hydrothermal treatment and tyrosinase: A circular dichroism spectrum, fluorescence, and molecular docking study. *Food Bioscience, 48*, Article 101790. https://doi.org/10.1016/j.fbio.2022.101790

Yu, Q., Fan, L., & Duan, Z. (2019). Five individual polyphenols as tyrosinase inhibitors: Inhibitory activity, synergistic effect, action mechanism, and molecular docking. *Food Chemistry, 297*, Article 124910. https://doi.org/10.1016/j.foodchem.2019.05.184

Zhang, L., Liu, Y., Wang, Y., Xu, M., & Hu, X. (2018). UV–Vis spectroscopy combined with chemometric study on the interactions of three dietary flavonoids with copper ions. Food Chemistry, 263: 208-215. https://doi.org/10.1016/j.foodchem.2018.05.009

Zhang, X., Yu, M., Zhu, X., Liu, R., & Lu, Q. (2022). Metabolomics reveals that phenolamides are the main chemical components contributing to the anti-tyrosinase activity of bee pollen. *Food Chemistry, 389*, Article 133071. https://doi.org/10.1016/j.foodchem.2022.133071

Zheleva-Dimitrova, D., Zengin, G., Sinan, K. I., Yıldıztugay, E., Mahomoodally, M. F., Ak, G., Picot-Allain, M. C. N., & Gevrenova R. (2020). Identification of bioactive compounds from *Rhaponticoides iconiensis* extracts and their bioactivities: An endemic plant to Turkey flora. *Journal of Pharmaceutical and Biomedical Analysis*, 190, Article 113537. https://doi.org/10.1016/j.jpba.2020.113537